ARTICLE
Traditional Medicine Research 2025;10(7):38. https://doi.org/10.53388/TMR20240520001

Investigation on the mechanism of Qi-Hong-Tang-Zu ointment in the treatment of diabetic wound by network pharmacology and experimental validation

Xian-Ce Che[1], Xiang-Mei Xiong[1], Zheng Liu[2], Peng-Wang Wang[2], Xia Li[2*], Wen-Yuan Gao[1, 2*]

[1]School of Traditional Chinese Materia Medica, Tianjin University of Traditional Chinese Medicine, Tianjin 301600, China. [2]Tianjin Key Laboratory for Modern Drug Delivery & High-Efficiency, School of Pharmaceutical Science and Technology, Faculty of Medicine, Tianjin University, Tianjin 300193, China.

[*]**Correspondence to:** Xia Li, Wen-Yuan Gao. Tianjin Key Laboratory for Modern Drug Delivery & High-Efficiency, School of Pharmaceutical Science and Technology, Faculty of Medicine, Tianjin University, No. 92, Weijin Road, Tianjin 300193, China. E-mail: lixia2008@tju.edu.cn; pharmgao@tju.edu.cn.

Author contributions

Che XC performed the experiment and wrote the manuscript. Xiong XM performed the data analyses. Liu Z and Wang PW were involved in interpretation and data collection. Li X and Gao WY contributed to the conception of the study.

Competing interests

The authors declare no conflicts of interest.

Acknowledgments

This work was financially supported by the Innovation Team and Talents Cultivation Program of National Administration of Traditional Chinese Medicine, (No. ZYYCXTD-D-202005). Tianjin Municipal Science and Technology Committee (20YFZCSY00560), the Key project at central government level (No. 2060302) and National Natural Science Foundation of China (No. 82373982, 82173969).

Peer review information

Traditional Medicine Research thanks Xue-Ping Yang and other anonymous reviewers for their contribution to the peer review of this paper.

Abbreviations

ELISA, enzyme-linked immunosorbent assay; KEGG, Kyoto Encyclopedia of Genes and Genomes; PPI, protein-protein interaction; TCM, traditional Chinese medicine; QHTZO, Qi-Hong-Tang-Zu ointment; HACAT, immortalized human epidermal cells.

Citation

Che XC, Xiong XM, Liu Z, Wang PW, Li X, Gao WY. Investigation on the mechanism of Qi-Hong-Tang-Zu ointment in the treatment of diabetic wound by network pharmacology and experimental validation. *Tradit Med Res.* 2025;10(7):38. doi: 10.53388/TMR20240520001.

Executive editor: Xin-Yue Zhang.

Received: 20 May 2024; **Revised:** 26 September 2024; **Accepted:** 21 January 2025; **Available online:** 24 January 2025.

Abstract

Background: Modern medical research has shown that Buyang Huanwu Tang and Taohong Siwu Tang have anti-inflammatory, analgesic, and microcirculation-improving effects, which can effectively promote wound healing in diabetic wounds. Qi-Hong-Tang-Zu ointment (QHTZO) is a modified prescription of Buyang Huanwu Tang and Taohong Siwu Tang; and has the function of removing necrotic tissue and promoting granulation and swelling-dispersing and pain-relieving. However, the effect of QHTZO in the treatment of diabetic wound is still unclear. The main objective of this study is to identify the effective components of QHTZO and investigate its wound healing activity in diabetic wound. **Methods:** UPLC-Orbitrap-MS/MS was utilized to analyze the active compounds of QHTZO. We conducted PPI, GO enrichments and KEGG pathway enrichment analyzes to understand the potential mechanisms of action of the QHTZO. Molecular docking analysis was performed to explore the interactions between the core components and their corresponding target proteins. The wound healing activity of the formula in diabetic wound was observed using ELISA, hematoxylin, and eosin staining and immunohistochemistry. **Results:** A total of 51 components of QHTZO were identified via UPLC-Orbitrap-MS/MS. *AKT1*, *TNF*, and *IL6* were identified as potential drug targets, and they were associated with PI3K/Akt signaling pathway and IL-17 signaling pathway. The molecular docking analysis has confirmed that ellagic acid, myricetin, and kaempferol have high affinity with the core target *IL6*. Histological results showed that QHTZO can promote collagen deposition, re-epithelialization, and induced angiogenesis and hair follicle regeneration, leading to wound healing. QHTZO can also reduce the expression of CD68, increase the expression of CD163, and induce macrophage polarization towards the M2 phenotype. ELISA experiments revealed that QHTZO can effectively increase the expression levels of IL-10 and TGF-β while decreasing the expression levels of TNF-α and IL-1β. **Conclusion:** QHTZO can effectively promote the repair of wound in diabetic rats by enhancing collagen deposition, regulating macrophage polarization, and reducing inflammation.

Keywords: network pharmacology; molecular docking; QHTZO; diabetic wound

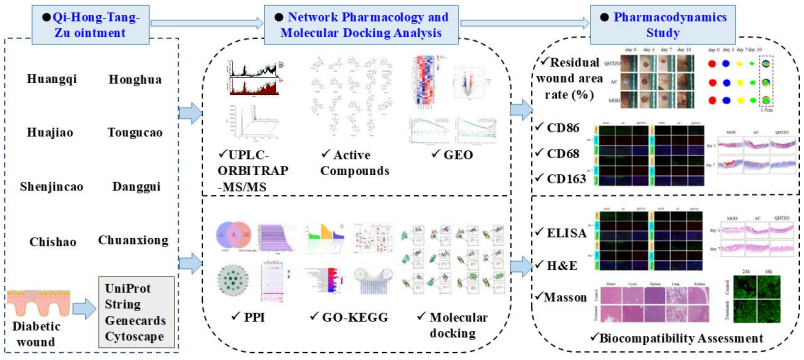

Highlights

Qi-Hong-Tang-Zu ointment accelerates wound healing by promoting the proliferation of wound tissue cells.
Qi-Hong-Tang-Zu ointment enhances wound contraction rates through facilitating collagen deposition.
Qi-Hong-Tang-Zu ointment modulates macrophage polarization, thereby alleviating the proinflammatory state in vivo and promoting wound healing.

Medical history of objective

The Taohong Siwu Decoction was first documented in *Yi Lei Yuan Rong* (compiled in 1291 C.E.) by Haogu Wang of the Yuan Dynasty, and later quoted in *Yu Ji Wei Yi* (compiled in 1396 C.E.), Volume 31, by Yanchun Xu of the Ming Dynasty. Its primary efficacy lies in nourishing blood, promoting blood circulation, and alleviating blood stagnation-induced pain. Modern research has revealed that the Taohong Siwu Decoction exhibits a multitude of pharmacological effects, including anti-inflammatory properties, hypolipidemic effects, vasodilation, antifatigue capabilities, resistance to hypoxia, anti-shock actions, and enhancement of immune function.

Introduction

Diabetes mellitus (DM) is a metabolic disease characterized by elevated blood glucose levels due to impaired insulin function [1]. The global prevalence of diabetes has been gradually increasing due to improvements in living standards and changes in dietary habits [2]. Approximately 463 million people worldwide were estimated to have diabetes [3]. Although diabetes can be well-controlled with appropriate management, it can lead to many complications such as vascular disorders, neuropathy, diabetic nephropathy, immune disorders, and diabetic wound (DW) [4]. It is estimated that around 19–34% of diabetic patients develop complications, including diabetic wound [5]. DW are characterized by a high rate of amputation, recurrence, and mortality, severely impacting the health and quality of life of patients [6, 7]. Currently, the treatment and care of diabetic wound have become significant challenges for healthcare systems worldwide.

Normal wound healing goes through four gradually recovering stages: hemostasis, inflammation, proliferation, and tissue remodeling [8]. However, chronic wounds such as venous ulcers, arterial ulcers, pressure ulcers, and diabetic ulcers tend to stall in the inflammatory phase. Macrophages play a crucial role in this process, with their anti-inflammatory (M2) polarization contributing to wound healing. However, damage to the inflammatory environment can disrupt the transition of macrophages from pro-inflammatory (M1) to M2, and diabetic patients and animals exhibit an increased M1/M2 ratio in their skin [9, 10]. Additionally, macrophages and neutrophils produce a large amount of ROS in response to hyperglycemic reactions during the inflammatory stage [11]. The lack of blood vessels around the wound further promotes ROS production. Excessive ROS, in turn, induces a strong inflammatory response, inhibits angiogenesis, and further deteriorates wound tissue [12, 13]. In summary, imbalances in redox levels, excessive expression of pro-inflammatory cytokines, abnormal differentiation of macrophages, bacterial infections, and sustained high glucose stimulation keep the wound in a persistent inflammatory microenvironment, severely interfering with neovascularization and tissue regeneration. This ultimately prolongs the healing time of the wound and increases the risk of infection and amputation.

Currently, the main approach to enhancing the clinical management of chronic wounds is through the local administration of growth factors. For example, the local application of rhGM-CSF and rhPDGF-BB has shown positive effects on wound healing. However, larger randomized controlled clinical trials are still needed to evaluate the efficacy of these growth factors in other types of ulcers [14]. Overall, current clinical therapies for diabetic wounds include debridement, antibiotics, glycemic control, and living skin transplantation, primarily focusing on preventing initial wound expansion and infection. However, they still cannot effectively promote diabetic wound regeneration, and 10% of diabetic wound patients ultimately undergo amputations [15, 16].

Traditional medicine plays an important role in the treatment and management of chronic wounds and wound healing processes. The use of traditional Chinese medicine (TCM) in wound treatment can be traced back to ancient times. According to ancient Chinese medical monographs, various herbal medicines in TCM were recommended for treating wounds [17]. Over time, significant progress has been made in demonstrating the wound healing activity of these herbal medicines and elucidating their underlying mechanisms [18].

The classical prescription, Modified Taohong Siwu Decoction, which comprises of *Angelicae Sinensis Radix* (Danggui) 20 g, *Chuanxiong Rhizoma* (Chuanxiong) 10 g, *Paeoniae Radix Rubra* (Chishao) 15 g, *Rehmanniae Radix* (Dihuang) 30 g, *Persicae Semen* (Taoren) 15 g, *Carthami Flos* (Honghua) 15 g, *Astragali Radix* (Huangqi) 30 g, *Codonopsis Radix* (Dangshen) 30 g, *Polygonati Rhizoma* (Huangjing) 50 g, and *Lycii Fructus* (Gouqizi) 20 g, exhibits a remarkable therapeutic effect on diabetic peripheral neuropathy. Based on this formulation, QHTZO was developed. QHTZO is composed of 8 Chinese herbal medicines including *Astragali Radix* (Huangqi), *Carthami Flos* (Honghua), *Zanthoxyli Pericarpium* (Huajiao), *Herba Speranskiae Tuberculatae* (Tougucao), *Lycopodii Herba* (Shenjincao), *Angelicae Sinensis Radix* (Danggui), *Chuanxiong Rhizoma* (Chuanxiong), and *Paeoniae Radix Rubra* (Chishao), and has the function of removing putrid tissues and promoting the growth of new tissues and dispersing swelling and relieving pain. Jingwan Hong ointment is a pure Chinese medicine preparation composed of more than 30 Chinese herbs such as *Angelicae Sinensis Radix* (Danggui), *Carthami Flos* (Honghua), *Paeoniae Radix Rubra* (Chishao), and *Chuanxiong Rhizoma* (Chuanxiong), with the efficacy of activating blood cir-culation to dissipate blood stasis, eliminating dampness by cooling, and detumescence by detoxification. Jingwan Hong ointment can up-regulate the expression of *PDGF* mRNA in the wounds of diabetic foot ulcers in rats, effectively promoting ulcer healing through tissue regeneration and angiogenesis [19]. Naoxin Tong capsules (NXT) is a Chinese medicine preparation composed of 16 Chinese herbs including *Astragali Radix* (Huangqi), *Paeoniae Radix Rubra* (Chishao), *Angelicae Sinensis Radix* (Danggui), *Chuanxiong Rhizoma* (Chuanxiong), and *Carthami Flos* (Honghua). Experimental results have shown that NXT increases collagen deposition and extracellular matrix production, reduces neutrophil infiltration, enhances M2 macrophage polarization and cell proliferation, reduces wound inflammation, improves wound healing rate, and accelerates wound repair progression [20].

However, there are still deficiencies in the efficacy evaluation and clinical application promotion of Chinese herbal compound formulations. In this experiment, QHTZO was used to treat diabetic wounds in rats by topical administration. The healing ability of QHTZO on wounds was observed, and further validation of the mechanism of action of QHTZO in treating diabetic wounds was performed using immunohistochemistry and immunofluorescence techniques, providing a molecular biology basis for its treatment of diabetic wounds.

Materials and methods

Preparation of the Chinese medicine compound extract

Chinese herbal medicine (*Astragali Radix* (Huangqi) 30 g, *Carthami Flos* (Honghua) 15 g, *Zanthoxyli Pericarpium* (Huajiao) 10 g, *Herba Speranskiae Tuberculatae* (Tougucao) 30 g, *Lycopodii Herba* (Shenjincao) 30 g, *Angelicae Sinensis Radix* (Danggui) 15 g, *Chuanxiong Rhizoma* (Chuanxiong) 10 g, *Paeoniae Radix Rubra* (Chishao) 15 g were purchased from Tongshuntang, Anhui, China) was soaked in 10-fold aqueous methanol for 1 h and decocted for 1 h. For the second

decoction, 10-fold aqueous methanol was added once again, and the solution was decocted for 1 h. Subsequently, the Chinese medicine compound extract was filtered and concentrated. The herbal medicine samples were blended with glycerol, glyceryl monostearate, liquid paraffin, and white petrolatum to prepare an ointment. The resulting QHTZO ointment contained 0.33 g/g (crude drug/ointment) of crude drug, and the dosage for each group was standardized at 0.1 g/cm^3.

Sample preparation for UPLC-Orbitrap-MS/MS

The 200 mg Chinese herbal medicine sample was dissolved in 50 mL of 70% aqueous methanol for 1 h and transferred into the ultrasonic machine for 0.5 h. Subsequently, the sample was centrifuged at 3,000 rpm for 20 min at 4 ˚C, and and filter through a 0.22 μm microporous membrane. The supernatant was subjected to UPLC-Orbitrap-MS/MS (Thermo Fisher Scientific, Waltham, MA, USA). Mobile phase A comprised acetonitrile, and phase B consisted of an aqueous phase containing 0.1% formic acid, with a flow rate of 0.25 mL/min. Throughout the procedure, the column temperature was maintained at 30 ˚C, and 5 μL of the injection fluid was used. The gradient program was as follows: 0–1 min, 90% B; 1–15 min, 90–10% B; 15–18 min, 10% B. The mass resolutions for precursor and fragment ions are 120,000 and 30,000 respectively. Other detailed ion source parameters are as follows: spray voltage, 3.5 kV for positive ions and 2.8 kV for negative ions; capillary temperature 320 ˚C; sheath gas flow rate (arb), 40; auxiliary gas flow rate (arb), 10; probe heater temperature, 350 ˚C; mass range (m/z), 100–1,200.

Network pharmacology and molecular docking

Active compounds and corresponding drug targets collection. Based on the results of the previous study and the above UPLC-Orbitrap-MS/MS analysis, the ADME (Absorption, Distribution, Metabolism, Excretion) model of basic drugs was screened using the SWISSADME (http://www.swissadme.ch/) database, and "Drug-likeness (DL) ≥ 0.18" was set as the screening index to obtain the main active ingredients in the QHTZO. SWISS target prediction (http://www.swisstargetprediction.ch/) was used as an online database to predict the targets of the main active ingredients in the QHTZO, and the obtained targets were sorted, combined, and de-weighted to obtain the regulatory targets of the active ingredients in the QHTZO.

Diabetic wound targets collection. We obtained the data of GSE68183 from GEO (https://www.ncbi.nlm.nih.gov/geo/) database and used R language, set $P < 0.05$, $|\log_2(\text{foldchange})| > 0.5$, and made volcano diagrams to collect the differential genes of the disease. The GeneCards (https://www.genecards.org/) database was searched for the key words "diabetic foot", "diabetic foot ulcer", "diabetic peripheral neuropathy", and "diabetic peripheral vascular disease" in the GeneCards database to search for diabetic wound-associated targets, and the obtained targets were sorted out and then combined and de-emphasized to obtain Diabetic wound-related targets.

Drug-disease common targets collection. Obtaining diabetes wound-related disease targets using GEO differential genes, GeneCards, DisGeNET (https://www.disgenet.org/), and OMIM (http://www.omim.org/) databases, respectively, and retaining unique values after merging, the disease-related genes for diabetes wound were obtained. By using Venny 2.1.0 (https://bioinfogp.cnb.csic.es/tools/venny/), the intersection of the drug's effective ingredient targets and the diabetes wound targets was obtained, which represents the potential target for QHTZO in treating diabetes wound.

Protein-protein interaction (PPI) network construction and selection of core targets. Import the intersection targets into the STRING (https://cn.STRING-db.org/cgi/) database for PPI analysis. Save the database in TSV format and import it into Cytoscape 3.7.2. Determine the node diameter and color depth based on the node degree value and screen the core targets.

Enrichment analysis of core targets. Import the genes of core targets for the effective ingredients in treating diabetes wound into the DAVID database (https://david.ncifcrf.gov). Set the species as "Homo sapiens" and perform Gene Ontology (GO) annotation and Kyoto Encyclopedia of Genes and Genomes (KEGG) pathway enrichment analysis. Load the data into a bioinformatics website for visualization.

Construction of a network for QHTZO-diseases-active ingredients-potential targets-pathways. Import nodes of QHTZO, active ingredient, target, disease, and the top 20 signaling pathways of the corresponding types into Cytoscape 3.7.2 to construct a "QHTZO-diseases-active ingredients-potential targets-pathways" network. This network aims to determine the potential mechanism of effective components in QHTZO for treating diabetes wounds.

Molecular docking. Perform molecular docking validation between the identified major active ingredients and core targets. Firstly, download the 2D structure file in sdf. Format of the major active ingredients from the PubChem (https://pubchem.ncbi.nlm.nih.gov/) database. Secondly, download the 3D structure file in PDB format of the core target proteins from the PDB (http://www.RCSB.org/) database. Further, use Discovery Studio 2019 software to process the protein and ingredient data, including hydrogenation, dehydration, and visualization of results.

Diabetic wound healing ability of QHTZO in a rat model

Diabetic wound rat model establishment and in vivo wound healing evaluation. The experimental animals consisted of 30 male SPF-grade Sprague-Dawley rats, which were supplied by the Tianjin Jinke Bona Biotechnology Co., Ltd. (No. SYXK (Jinbin) 2023-0005). All animal treatment and experiments were approved by the Animal Ethics Committee of the Tianjin Jinke Bona Biotechnology Co., Ltd. (No. GENINK-20230048). According to the guidelines for the care and use of experimental animals of the National Institute of Health, the animal welfare is closely monitored. Before modeling, male SD rats (6–8 weeks and weight 180–220 g) were fasted for 12 h without water restriction, followed by intraperitoneal injection of streptozotocin (STZ, 50 mg/kg body weight). The blood glucose levels of the rats were monitored using a glucose meter after 2 weeks. An indication of a successful establishment of the diabetes model was noted when the blood glucose level exceeded 16.7 mmol/L. Full-thickness diabetic wounds were created on the backs of the rats using a 1 cm diameter punch biopsy device. The rats were randomly divided into three experimental groups (n = 10 in each group) and covered with 100 μL of PBS (MOD), Shengji ointment (SJO, active control, AC), and QHTZO, respectively. Digital images of the wounds were captured at specific time points, and the remaining wound area (%) was assessed through the tracing of wound boundaries in each group. The residual wound area rate was determined using the Equation (1):

$$\text{Residual wound area rate (\%)} = [\text{Wound healing area (n day)}/\text{Original wound area}] \times 100 \quad (1)$$

Where "n" represents the time points of 0, 3, 7, and 10 d.

Histology and immunohistochemical staining. On day 3 and 7 after injury, diabetic rats were sacrificed, and the wounded tissues were immediately fixed in 4% paraformaldehyde. After 24-h dehydration, the tissue samples were embedded in paraffin, transversely sectioned at approximately 5 μm thickness for hematoxylin and eosin (H&E) and Masson's trichrome staining. Moreover, immunohistochemical staining was performed on the tissue slices.

ELISA isolation assessment. The rats were sacrificed at scheduled time points to analyze cytokine levels using ELISA kits (Beijing Solarbio Science & Technology Co., Ltd. Beijing, China) on the wound tissues. ELISA kits were utilized to measure *TNF-α*, *IL-6*, and *IL-1β* levels in serum, following the manufacturer's instructions.

Statistical analysis

Data analysis was carried out using GraphPad Prism software. Prism 8.0.2 was employed for statistical analysis, with a one-way analysis of variance utilized to assess the significance of the results. All results were shown as the mean ± standard deviation, and at least three independent repeated experiments were performed. A significance level of $P < 0.05$ was deemed statistically significant.

Results

Analysis of active compound in TCM formula

UPLC-Orbitrap-MS/MS analysis yielded a total of 51 active compounds, with 29 compounds detected in positive ion mode and 22 in negative ion mode. Table 1 provides detailed information on the chemical names, retention times, molecular weights, molecular formulas, and other characteristics of these 51 active compounds.

Screening of active compounds and target identification

Using DL ≥ 0.18 and drug ADMET (Absorption, Distribution, Metabolism, Excretion, Toxicity) condition as the screening criterion, a total of 18 compounds were identified as potential active components in the TCM formula (Supplementary Table S1, Figure 1). The TCMSP database and SWISS target prediction database were employed to predict the targets regulated by these 18 compounds, resulting in 1,278 potential targets. After removing duplicate targets and standardizing target names using Uniprot, and discarding targets that could not be identified, a total of 433 regulatory targets of active ingredients extracted from Chinese herbal compound extracts were obtained.

Obtaining targets related to diabetic wounds

The GeneCards database was searched using the keywords “Diabetic Foot”, “Diabetic foot ulcer”, “diabetic peripheral neuropathy”, and “diabetic peripheral vascular disease” to identify targets associated with diabetic wound. After removing duplicates, a total of 10,452 targets related to diabetic wound were obtained. The GSE68183 dataset was retrieved from the GEO database, and R language was used for data normalization and differential analysis. Differential gene heatmaps and volcano plots were generated (Figure 2A, 2B). A total of 250 differentially expressed genes were identified, with 107 genes upregulated and 143 genes downregulated in diabetic wound. The obtained targets were merged and organized, and duplicates were removed, resulting in a final list of 10,579 targets related to diabetic wound.

Table 1 The components of Chinese medicine compound was identified by UPLC-Orbitrap-MS/MS in both positive and negative

No.	RT (min)	Ion mode	Experimental Mass m/z	Error (ppm)	MS^2 (m/z)	Formula	Component name
1	23.138	$[M-H]^-$	442.37760	−7.87	107.08523, 121.10062, 133.10043, 425.37479	$C_{30}H_{50}O_2$	α-Onocerin
2	21.699	$[M-H]^-$	458.37233	−7.99	109.10084, 123.11620, 139.11084, 149.09528	$C_{30}H_{50}O_3$	Lycoclavano
3	21.602	$[M+H]^+$	270.25450	−5.10	103.07523, 117.09061	$C_{17}H_{34}O_2$	Daturic acid
4	21.159	$[M+H]^+$	281.26964	−7.37	154.07652, 218.24757, 247.23993, 265.25006	$C_{18}H_{35}NO$	ELD
5	21.026	$[M-H]^-$	456.35783	−5.51	107.08531, 121.10072, 151.11081, 439.35342	$C_{30}H_{48}O_3$	Mairin
6	20.750	$[M-H]^-$	166.02530	−7.88	105.06963, 121.02789, 123.11623, 139.11086, 149.02240	$C_8H_6O_4$	Isophthalic acid
7	19.772	$[M+H]^+$	303.25463	−5.24	105.06994, 114.09132, 147.11606, 170.15338, 218.21703, 248.19992	$C_{20}H_{33}NO$	Arachidonoyl amide
8	19.695	$[M-H_2O]^-$	262.22826	−4.38	107.08543, 109.10120, 123.11668, 245.22560, 263.23599	$C_{18}H_{32}O_2$	Linoleic acid
9	17.621	$[M-H]^-$	472.35252	−5.80	101.38459, 114.45409, 128.92249, 225.32127, 225.33253, 453.15930	$C_{30}H_{48}O_4$	Augustic-acid
10	15.789	$[M+Na]^+$	276.20757	−4.87	107.08559, 121.10101, 135.11639, 235.16837	$C_{16}H_{30}O_2$	Palmitoleic acid
11	10.777	$[M+H]^+$	316.05678	−4.82	153.01761, 229.04861, 245.04358, 257.04312, 273.03799, 285.03799, 302.04071	$C_{16}H_{12}O_7$	Isorhamnetin
12	10.765	$[M-H]^-$	330.23878	−5.57	139.11203, 171.10196, 183.13820, 199.13321, 211.13289, 229.14319, 311.22131	$C_{18}H_{34}O_5$	Pinellic acid
13	9.197	$[M+H]^+$	288.06188	−5.25	117.03333, 123.04390, 135.04359, 145.02776, 153.01762, 163.03830, 171.02821, 179.03320	$C_{15}H_{12}O_6$	6-Hydroxynaringenin
14	9.150	$[M-H]^-$	202.11937	−5.65	139.11214, 165.83572, 183.10167	$C_{10}H_{18}O_4$	3-tert-butylhexanedioic acid
15	9.124	$[M+H]^+$	462.11418	−4.39	153.01762, 218.90862, 229.04872, 246.05121, 257.04324, 285.03812, 302.04077, 317.06427	$C_{22}H_{22}O_{11}$	Pratensein-7-O-Glc
16	8.958	$[M-H]^-$	432.10323	−4.12	107.01334, 151.00290, 169.01337, 257.04443, 285.03906	$C_{21}H_{20}O_{10}$	Cosmosiin
17	8.940	$[M+H]^+$	146.03615	−4.31	105.07000, 119.04903, 129.06946	$C_9H_6O_2$	Coumarin
18	8.015	$[M-H]^-$	318.03563	−6.10	109.02889, 137.02367, 151.00285, 169.01344, 178.99763, 218.91615	$C_{15}H_{10}O_8$	Myricetin
19	7.895	$[M-H]^-$	188.10376	−5.85	116.99513, 123.08088, 143.10690, 159.87801, 166.99165	$C_9H_{16}O_4$	Azelaic acid
20	7.232	$[M+H]^+$	448.09862	−4.33	121.02824, 127.03870, 145.04884, 153.01764, 165.01741, 287.05377	$C_{21}H_{20}O_{11}$	Amoenin A3
21	6.771	$[M-H_2O]^-$	224.25300	−4.67	133.06438, 151.07472, 161.05910, 175.07474, 192.07735, 207.10083	$C_{12}H_{16}O_4$	Senkyunolide I
22	6.754	$[M-H]^-$	166.06201	−5.93	101.03916, 119.04959, 121.02882, 147.04437, 164.83505	$C_9H_{10}O_3$	Paeonol

Table 1 The components of Chinese medicine compound was identified by UPLC-Orbitrap-MS/MS in both positive and negative (*continued*)

No.	RT (min)	Ion mode	Experimental Mass m/z	Error (ppm)	MS^2 (m/z)	Formula	Component name
23	6.672	$[M+H]^+$	302.04112	−5.06	153.01770, 229.04865, 247.02283, 257.00702	$C_{15}H_{10}O_7$	Quercetin
24	6.671	$[M+H]^+$	464.09349	−4.27	165.01768, 201.05429, 229.04855, 257.04318, 303.04865	$C_{21}H_{20}O_{12}$	Quercimeritrin
25	6.625	$[M+H]^+$	302.00484	−4.73	137.02289, 153.01770, 201.01755, 229.04865, 247.02283, 257.00702, 285.00186	$C_{14}H_6O_8$	Ellagic acid
26	6.484	$[M-H]^-$	164.04640	−5.75	119.01305, 135.04451, 145.02896	$C_9H_8O_3$	Cis-4-coumaric acid
27	6.348	$[M+H]^+$	610.14928	−4.68	137.02249, 153.01744, 222.76682, 229.04823, 303.04773, 449.10538	$C_{27}H_{30}O_{16}$	Kaempferol 3-O-β-sophoroside
28	6.139	$[M+H]^+$	386.10109	2.39	107.08520, 132.95752, 174.96774, 219.66144, 225.05588, 234.98837, 267.06586, 279.06592, 369.09723	$C_{20}H_{18}O_8$	Phrymarolin V
29	6.016	$[M+H]^+$	286.04640	−4.66	121.02789, 137.02245, 153.01723, 165.01723, 183.02759, 213.05315, 241.04794, 258.05057	$C_{15}H_{10}O_6$	Kaempferol
30	6.015	$[M+H]^+$	594.15453	−5.15	121.02782, 153.01735, 165.01683, 287.05295, 433.10986	$C_{27}H_{30}O_{15}$	Nicotiflorin
31	5.981	$[M-H]^-$	480.08757	−5.88	178.99745, 214.02605, 242.02049, 270.01630, 287.01785, 316.02063	$C_{21}H_{20}O_{13}$	Tagetiin
32	5.889	$[M-H_2O]^-$	125.08338	−4.63	108.08051, 126.05432	$C_7H_{13}NO_2$	DL-Threonine
33	5.817	$[M-H]^-$	154.02574	−5.64	110.03226, 135.00813	$C_7H_6O_4$	Protocatechuic acid
34	4.785	$[M-H]^-$	138.03088	−5.88	109.02898, 114.44559	$C_7H_6O_3$	Protamine sulfates
35	4.509	$[M-H]^-$	290.07756	−5.10	109.02888, 123.04463, 137.02379, 151.03918, 203.07045, 245.00781	$C_{15}H_{14}O_6$	Epicatechin
36	3.658	$[M-H]^-$	484.08262	−5.54	125.02370, 168.00545, 193.01314, 211.02373, 218.49788, 271.04456, 313.05496	$C_{20}H_{20}O_{14}$	Galloylglucose
37	2.106	$[M+H]^+$	165.07800	−5.90	103.05413, 107.04896, 120.08037, 138.05418, 166.08549	$C_9H_{11}NO_2$	Phenylalanine
38	1.919	$[M-H]^-$	170.02057	−5.62	107.01331, 125.02377	$C_7H_6O_5$	Gallic acid
39	1.880	$[M+H]^+$	126.03108	−4.90	109.02815	$C_6H_6O_3$	5-(Hydroxymethyl)furan-2-carbaldehyde
40	1.773	$[M+H]^+$	267.09511	−6.15	119.03484, 137.04515, 224.45299	$C_{10}H_{13}N_5O_4$	ADO
41	1.773	$[M+H]^+$	131.09395	−5.17	104.04916	$C_6H_{13}NO_2$	D-tert-Leucine
42	1.771	$[M-H]^-$	244.06798	−6.39	110.02418, 127.05061, 152.03455, 219.85860	$C_9H_{12}N_2O_6$	Uridine
43	1.718	$[M+H]^+$	296.26970	−6.17	247.24069, 266.99762, 283.02881	$C_{19}H_{36}O_2$	Exceparl M-OL
44	1.188	$[M-H]^-$	192.02597	−5.38	111.00822, 129.01872	$C_6H_8O_7$	Limonexic acid
45	1.150	$[M+H]^+$	115.06296	−3.21	98.03395	$C_5H_9NO_2$	Proline
46	1.143	$[M-H]^-$	192.06230	−5.67	111.00821, 127.03940	$C_7H_{12}O_6$	D- (-)-Quinic acid
47	1.135	$[M-Na]^-$	336.08003	−4.23	112.07550, 114.05465, 140.06998, 220.86884, 253.11659, 337.08759	$C_{16}H_{18}O_9$	Heriguard
48	1.134	$[M-H]^-$	268.07781	−4.36	105.01878, 113.02389	$C_{16}H_{12}O_4$	Formononetin
49	1.129	$[M+Na]^+$	364.09590	−6.10	101.37939, 114.44608, 138.05405, 155.26265, 173.36427, 185.04103, 203.05144, 220.58041, 302.70685	$C_{12}H_{22}O_{11}$	Sucrose
50	1.100	$[M+H]^+$	103.09954	−2.18	86.03747	$C_5H_{13}NO$	Choline
51	1.012	$[M+H]^+$	174.11070	−5.58	116.07027, 130.09686, 157.10742	$C_6H_{14}N_4O_2$	Argininic acid

ELD, Eldamic acid amide; ADO, Adenosine.

Traditional Medicine Research 2025;10(7):38. https://doi.org/10.53388/TMR20240520001

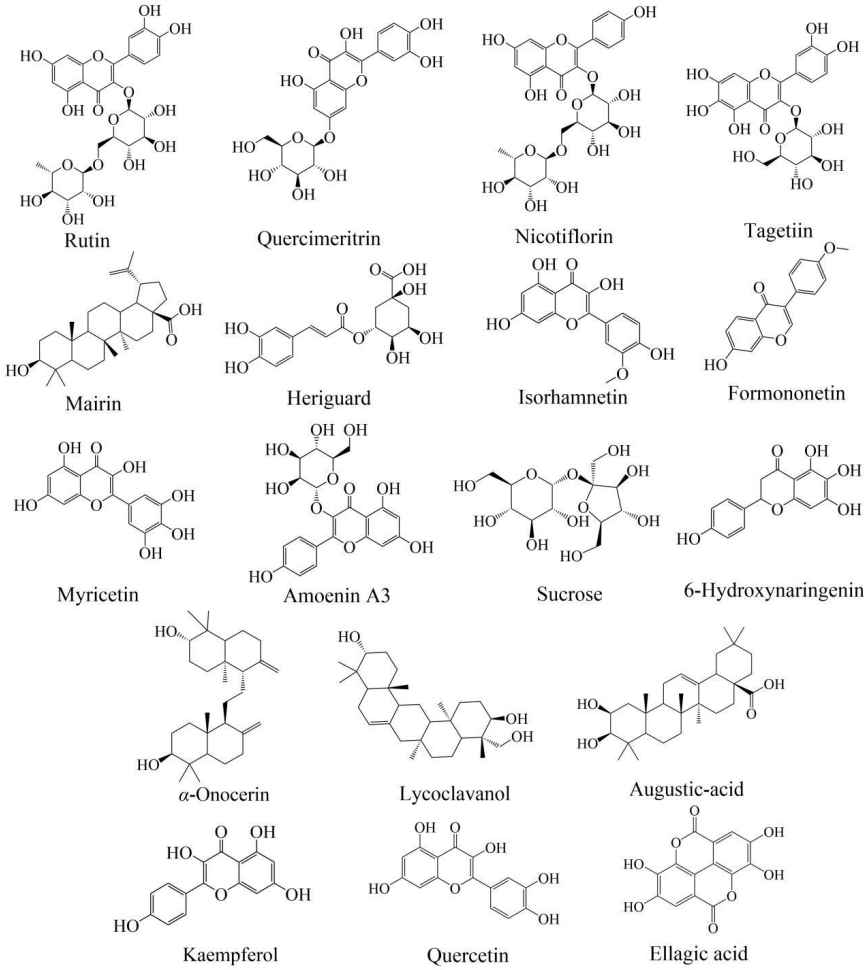

Figure 1 Chemical structure formula for core components.

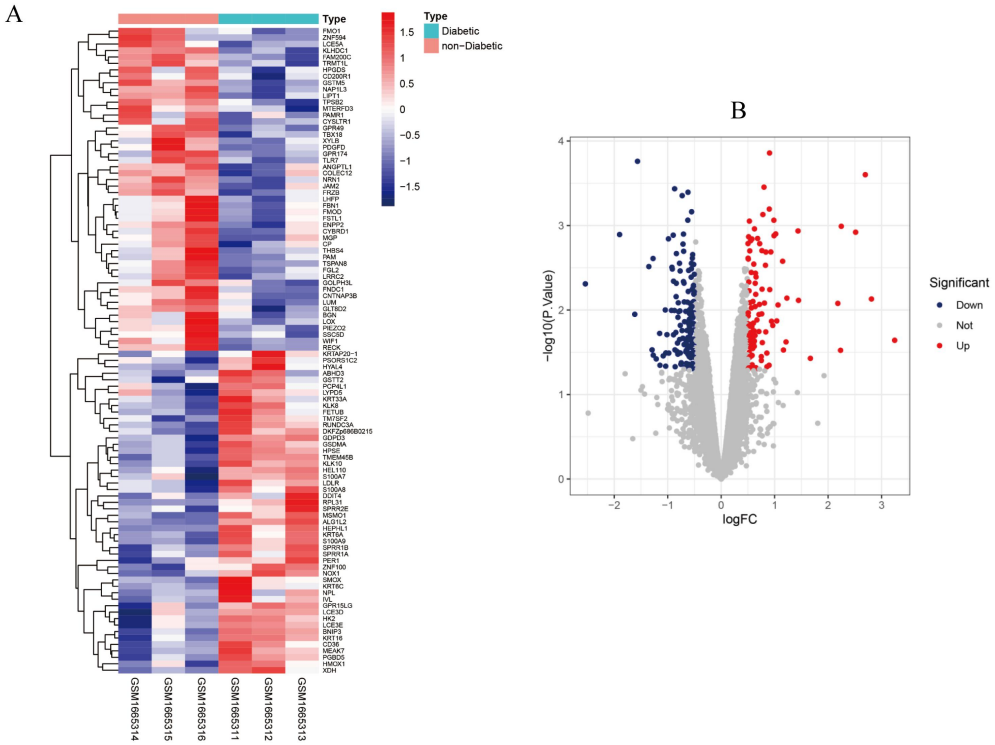

Figure 2 GEO data mining. (A) Diabetic wounds differential gene heat map; (B) GEO differential analysis volcano map.

After sequencing the differential genes of diabetic wound according to log_2FC, gene set enrichment analysis found that compared with normal people, upregulated genes were significantly enriched in glutathione metabolism, insulin signaling pathway, and PAPR signaling pathway, while downregulated genes were significantly enriched in cytokine receptor interaction, toll like receptor signaling pathway, and chemokine signaling pathway (Figure 3A, 3B).

Network pharmacology analysis

Intersection analysis using a Venn diagram was performed between the regulatory targets of active compounds in the TCM formula and targets related to diabetic wound, resulting in 401 common targets (Figure 4A). These 401 targets may represent potential therapeutic targets for treating diabetic wounds with the TCM formula. The PPI network of these 401 common targets was obtained using the STRING database, and core targets in key modules were selected based on their degree values (Figure 4B). Ten core targets were identified based on the degree values, namely *AKT1, TNF, IL6, TP53, IL-1β, SRC, EGFR, CASP3, STAT3, and MYC* (Figure 4C). These 10 core targets may be the key targets of QHTZO in the treatment of diabetic wounds.

GO and KEGG analyzes were performed on the 401 common targets using the David database (Figure 4D, 4E). The potential therapeutic targets of the TCM formula and diabetic wound were found to be involved in biological processes such as signal transduction, negative regulation of apoptotic process, and positive regulation of cell proliferation. They were associated with cellular components such as plasma membrane, cytosol, and cytoplasm, and molecular functions such as identical protein binding, ATP binding, and enzyme binding. The main enriched pathways identified in the KEGG analysis included PI3K-Akt signaling pathway, AGE-RAGE signaling pathway in diabetic complications, and IL-17 signaling pathway. The PI3K/Akt was searched using the KEGG database, and the potential targets of diabetic wound effects of active ingredients involved in this pathway were red flagged. The network diagram of the QHTZO-diseases-active ingredients-potential targets-pathways network was constructed using Cytoscape 3.7.2 (Figure 5). Analysis revealed that quercetin, kaempferol, and myricetin had high degree values, indicating that these compounds are likely core components for treating diabetic wounds.

Molecular docking

The top eight potential targets (*AKT1, TNF, IL-6, TP53, IL-1β, EGFR, CASP3,* and *STAT3*) with degree values in the PPI protein network were docked with the top eight active components (quercetin, kaempferol, myricetin, isorhamnetin, lycoclavanol, ellagic acid, formononetin, and 6-hydroxynaringenin) with degree values in the "QHTZO-diseases-active ingredients-potential targets-pathways network". The binding affinities of 64 docking poses are shown (Supplement Figure S1). The highest binding affinity of each molecule was visualized in Figure 6A–6D.

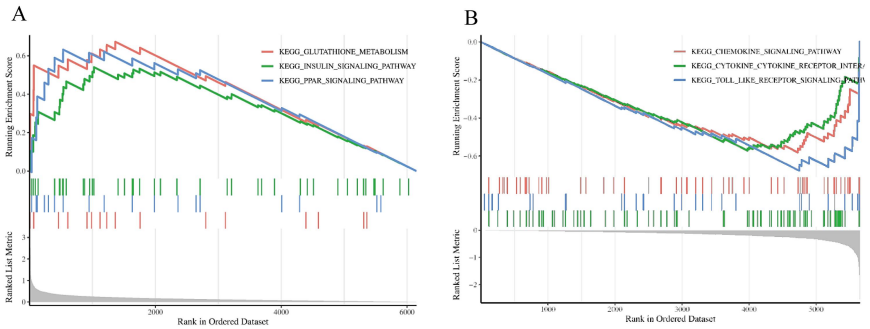

Figure 3 Gene enrichment analysis. (A) Up-regulated gene set analysis; (B) Down-regulated gene set analysis. KEGG, Kyoto Encyclopedia of Genes and Genomes.

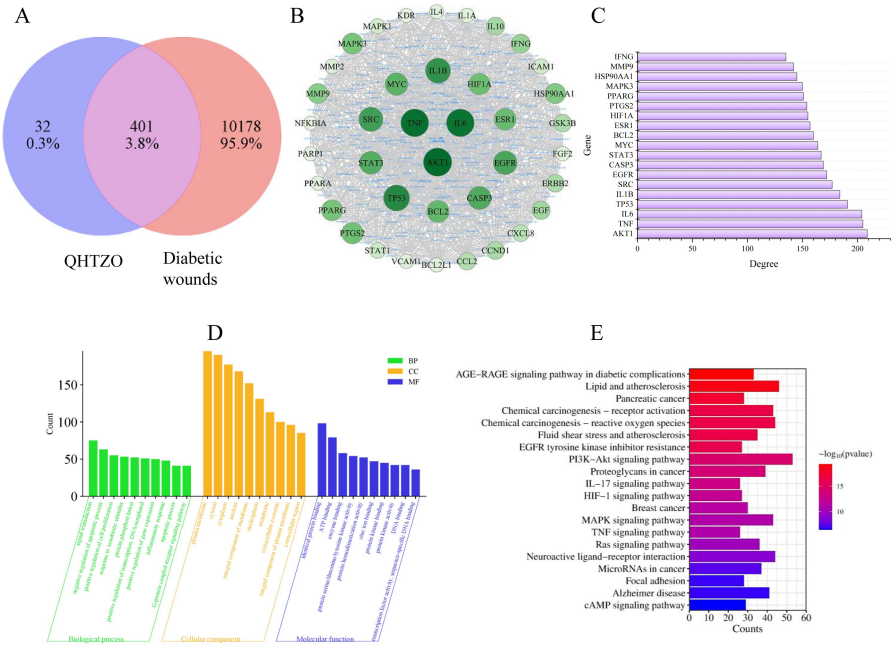

Figure 4 Network pharmacology analysis. (A) Venn diagram of component-disease targets; (B) PPI network diagram; (C) Core gene bar chart; (D) GO enrichment analysis; (E) KEGG pathway enrichment analysis of core targets. QHTZO, Qi-Hong-Tang-Zu ointment; BP, biological process; CC, cellular components; MF, molecular function.

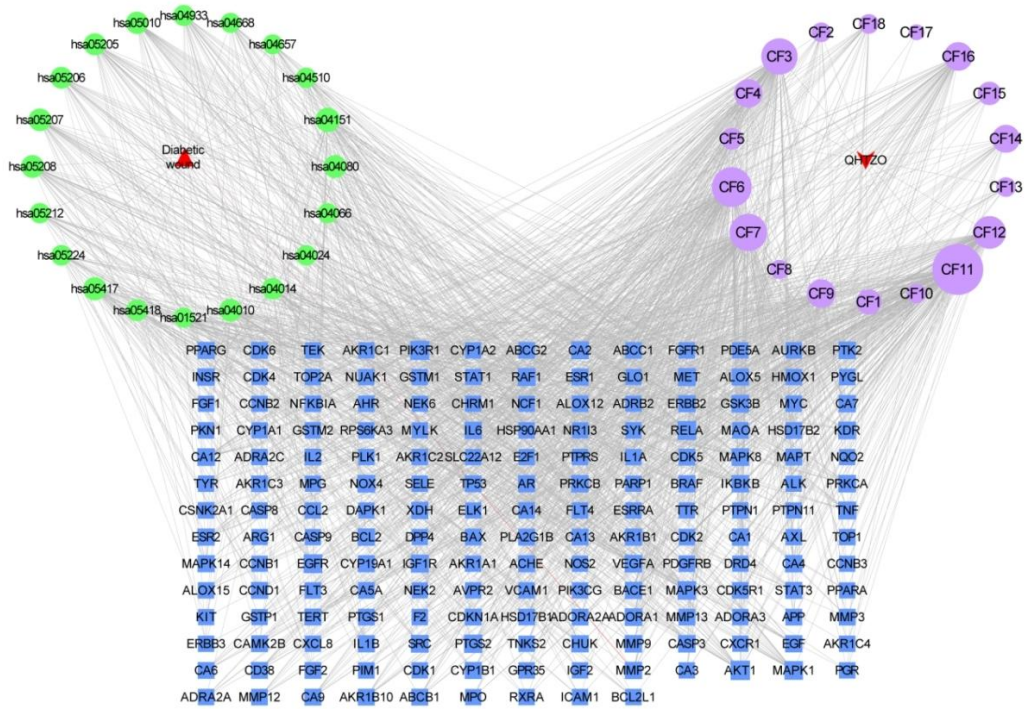

Figure 5 QHTZO-diseases-active ingredients-potential targets-pathways network. QHTZO, Qi-Hong-Tang-Zu ointment.

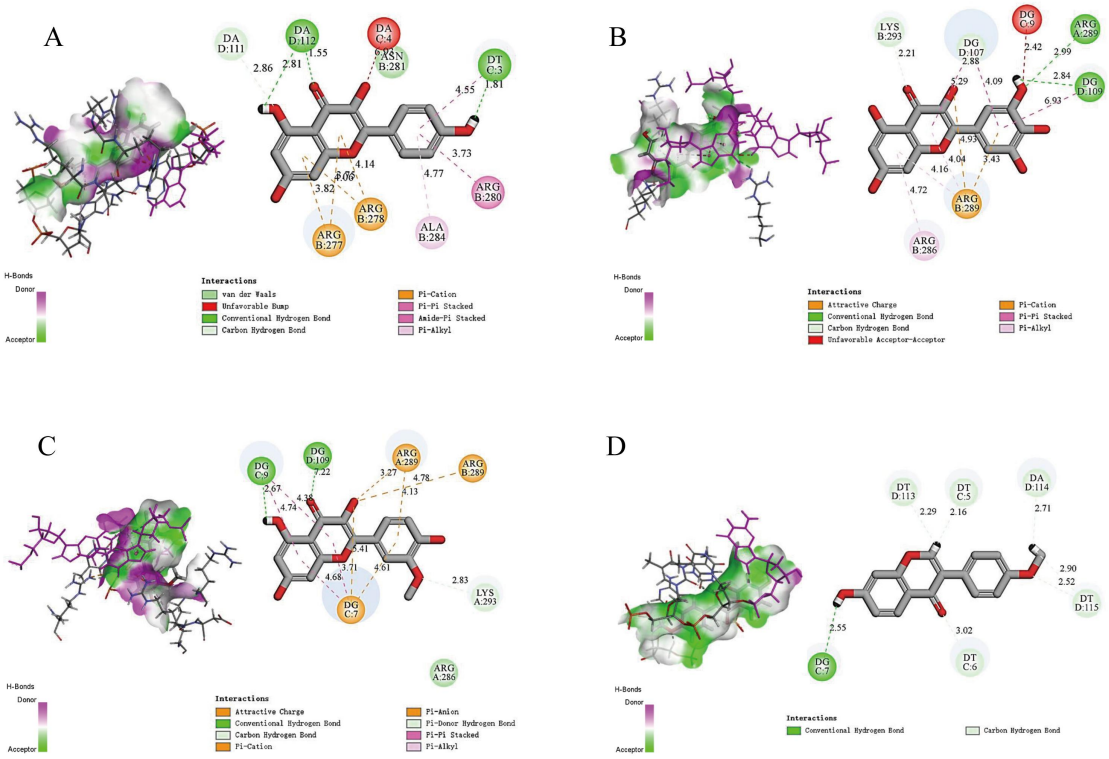

Figure 6 Molecular docking of active ingredients and core genes. (A) Kampferol-*IL6* (*6MG1*); (B) Myricetin-*IL6* (*6MG1*); (C) Isorhamnetin-*IL6* (*6MG1*); (D) Formononetin- *IL6* (*6MG1*).

Validation of pharmacological activity in vivo

Study on accelerated wound healing model in diabetic rats. A full-thickness skin wound model in diabetic rats induced by STZ was used to further investigate the tissue repair effects of a QHTZO in vivo. The wounds on diabetic rats were immediately treated with PBS, Shengji ointment, or QHTZO (Figure 7A). Digital photos of the wounds showed that the wound healing rate of the QHTZO group was the highest, reaching nearly 70% on the 10th day of treatment. It significantly promoted the wound healing speed in diabetic rats at all tested time points and reduced the wound healing time (Figure 7B, 7C). After 10 d of treatment, the wound healing rates of PBS group, Shengji ointment group, and QHTZO group were 53.99 ± 1.50%, 61.6 ± 1.38%, and 70.15 ± 2.19%, respectively (Figure 7D).

Traditional Medicine Research 2025;10(7):38. https://doi.org/10.53388/TMR20240520001

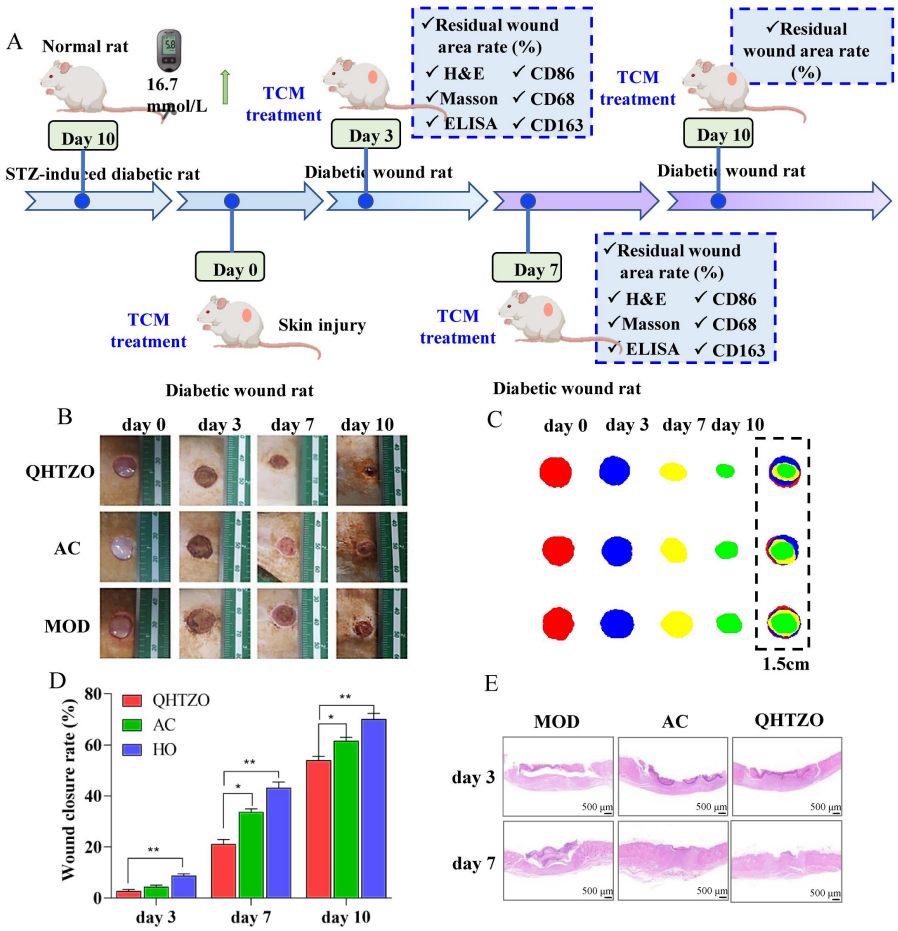

Figure 7 QHTZO accelerates wound closure in diabetic wound rats. (A) Flow diagram depicting the use of QHTZG in animal trials; (B) Representative photographs of diabetic wounds in different treatment groups; (C) Traces of wound healing process in different treatment groups; (D) Quantitative analysis of residual wound area on days 3, 7, and 10 after treatment in different groups (n = 3); (E) Morphological observation of diabetic wound area on day 3 and 7 stained with H&E in different groups (scale bar = 500 μm). $^{*}P < 0.05$, $^{**}P < 0.01$, compared with MOD group. TCM, traditional Chinese medicine; H&E, hematoxylin and eosin; ELISA, enzyme-linked immunosorbent assay; QHTZO, Qi-Hong-Tang-Zu ointment.

Subsequently, H&E examination of the wound healing quality was performed on the 3rd and 7th days. From the representative macroscopic view and skin wound simulation images of each group, it was found that the QHTZO group had good wound repair effects. Granulation tissue formation was more organized, inflammation cell infiltration was effectively reduced, and there was an increase in re-epithelialization thickness and faster wound healing compared to the Shengji ointment group. In the PBS group, there was excessive inflammation cell infiltration, formation of necrotic tissue, and limited regeneration of granulation tissue (Figure 7E).

Regulating macrophage polarization to alleviate pro-inflammatory state. In diabetic wounds, macrophages fail to effectively transition from the M1 to M2 phenotype due to factors such as accumulation of glycation end products and high blood sugar levels, leading to prolonged inflammation and oxidative stress. The experimental results showed that QHTZO could effectively induce macrophage polarization (Figure 8A). QHTZO can regulate macrophage polarization and alleviate pro-inflammatory effects. To determine whether the QHTZO affects macrophage polarization, dual positive immunofluorescence staining was performed on M1 and M2 macrophages. Confocal laser scanning microscopy images showed that the PBS group induced expression of CD86 (M1 macrophages), while the fluorescence intensity was relatively weaker in the positive control group and the QHTZO group, and the number of M1 macrophages was also lower (Figure 8B). Furthermore, compared to the PBS group, the expression of CD163 (M2 macrophages) was upregulated in the positive control group and the QHTZO, with higher levels in the QHTZO group (Figure 8C).

The activation state of macrophages has a significant impact on the wound healing process. To evaluate the anti-inflammatory effects of the QHTZO, an ELISA assay was performed on skin tissue samples collected from the wounds on post-treatment days 3 and 7. The results showed that the QHTZO significantly increased the expression of anti-inflammatory markers such as *IL-10* and *TGF-β* compared to the untreated control group (Figure 8D, 8E).

Previous studies have found a correlation between the excessive production of *IL-10* by M2 macrophages in streptozotocin-induced diabetic rats and the production of pro-inflammatory cytokines. Additionally, the QHTZO-treated group showed a significant reduction in inflammatory markers such as *TNF-α* and *IL-1β* levels compared to the untreated control group (Figure 8F, 8G).

Mechanisms promoting wound closure. To evaluate the effects of the QHTZO on skin regeneration, we used immunofluorescence staining to detect the expression of the cell proliferation marker Ki67. The wounds treated with the QHTZG displayed significantly enhanced Ki67 cell expression compared to the other groups, indicating that the QHTZO promotes cell proliferation in the harsh wound microenvironment (Figure 9A). To validate the activation of collagen metabolism, we assessed the expression of integrin α3 through immunofluorescence staining. The positive expression of integrin α3 was significantly increased in the QHTZO group, indicating collagen deposition and a more uniform distribution of collagen. These results further demonstrate the potential of the QHTZO in promoting skin cell proliferation and collagen synthesis (Figure 9B). Masson's trichrome

staining, which labels collagen, showed that the QHTZO group had the most abundant collagen deposition (Figure 9C).

Biocompatibility assessment. To evaluate the biocompatibility of the QHTZO, we conducted cell toxicity assays and observed histopathological tissue sections of visceral organs. Firstly, we examined the toxicity of the TCM extract on immortalized human epidermal cells (HACAT cells). We assessed HACAT cells cultured for 24 and 48 h using live/dead cell staining and confocal laser scanning microscopy. The experimental results showed that most of the HACAT cells in the treatment group appeared green (green cells indicating live cells, and red cells indicating dead cells), like the control group, indicating no significant toxicity of the TCM extract on cells (Figure 10A). Furthermore, on postoperative day 10, we conducted HE staining on the visceral organs of the different treatment groups and observed the tissue structure of the heart, liver, spleen, lungs, and kidneys. The results showed no significant structural changes or accumulation of inflammatory cells in these organs (Figure 10B). All these pieces of evidence suggest that the QHTZO has good biocompatibility.

Discussion

DM is an increasingly concerning public health issue worldwide, annually leading to non-healing ulcers, subsequent gangrene, and even necessitating amputation, seriously endangering human health [21–23]. The risk of ulcer recurrence is also remarkably high, with a 40% recurrence rate in the first year after healing, and a 65% recurrence rate within the following three years [24]. TCM plays a significant role in treating diabetic wounds, with plant chemical analysis indicating the presence of various compounds such as alkaloids, flavonoids, phenols, saponins, steroids, and tannins [25, 26]. It has been proven that TCM can promote diabetic wound healing by regulating signaling pathways including Wnt, NF-κB, Notch, PI3K/Akt/mTOR, TGF-β/Smad, IL-17, and MAPK, inhibiting oxidative stress, enhancing angiogenesis, increasing cytokine production, regulating abnormal glucose metabolism, promoting proliferation of keratinocytes and fibroblasts, and ultimately facilitating the healing of diabetic wounds [27].

QHTZO is a combination of modified Buyang Huanwu Tang and Taohong Siwu Tang, with the functions of promoting tissue regeneration, activating blood circulation, eliminating stasis, clearing heat, and detoxifying. In this study, UPLC-Orbitrap-MS/MS analysis was used to identify the chemical components in the TCM compound and a total of 51 compounds were identified, with 18 of them being the main components. The network pharmacological analysis was further conducted, and this study identified the top-ranked effective components as quercetin, ellagic acid, myricetin, kaempferol, tannic acid, and vitexin. These components have been reported to possess anti-inflammatory, antioxidant, antimicrobial, and wound healing properties.

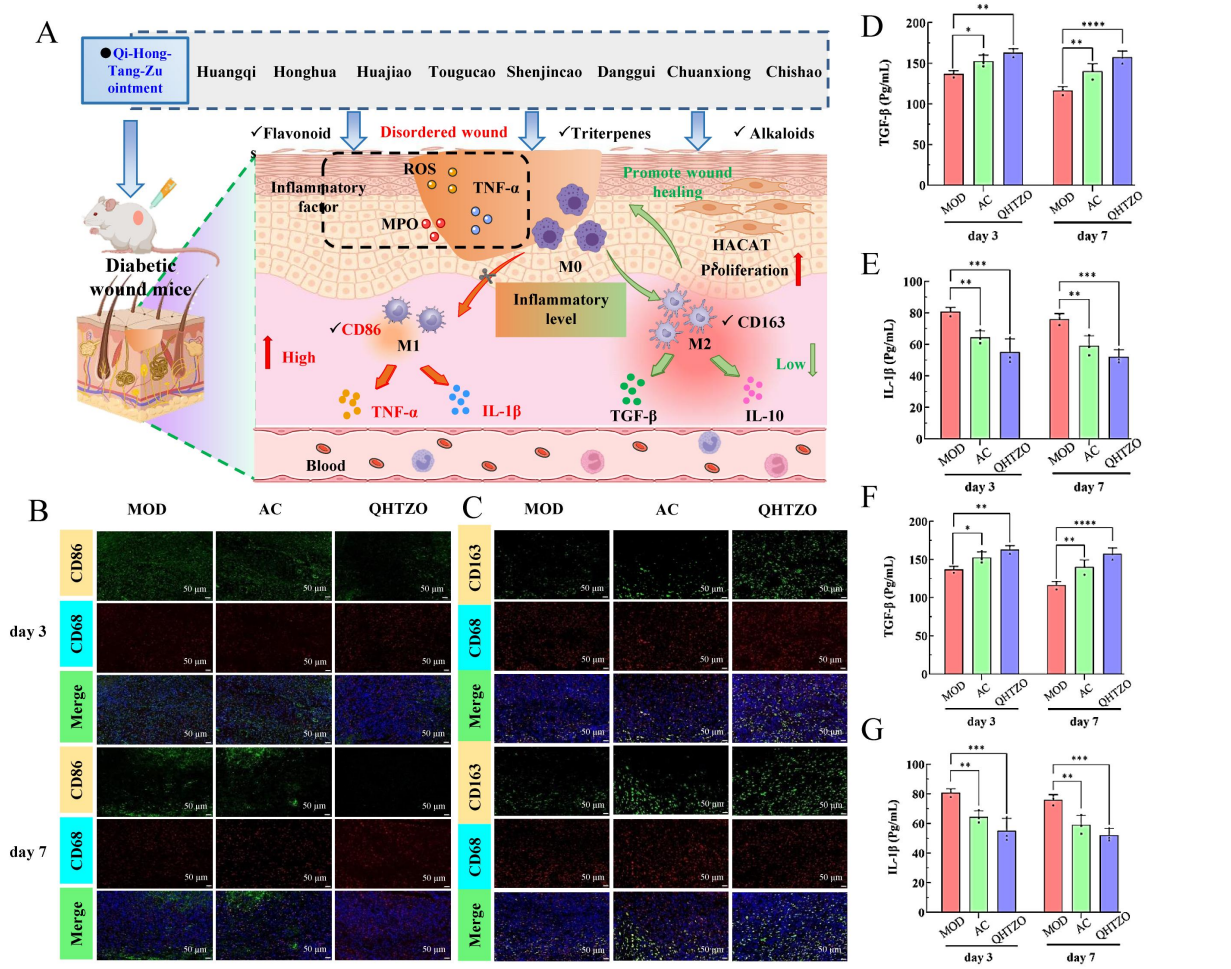

Figure 8 QHTZO regulates macrophage polarization and alleviates pro-inflammatory state in vivo. (A)The experimental results showed that QHTZO could effectively induce macrophage polarization; (B) Immunofluorescence staining of wound area in different groups labeled with CD86 (green), CD68 (red), and DAPI (blue) (scale bar = 50 μm); (C) Immunofluorescence staining of wound area in different groups labeled with CD163 (green), CD68 (red), and DAPI (blue) (scale bar = 50 μm); ELISA analysis of expression of (D) *TGF-β*, (E) *IL-10*, (F) *IL-1β*, and (G) *TNF-α* (n = 3). $^{*}P < 0.05$, $^{**}P < 0.01$, $^{***}P < 0.001$, $^{****}P < 0.0001$, compared with MOD group. QHTZO, Qi-Hong-Tang-Zu ointment; ROS, reactive oxygen species; MPO, myeloperoxidase; HACAT, immortalized human epidermal cells; TGF-β, transforming growth factor-β; IL-10, interleukin 10; IL-1β, interleukin 1β; TNF-α, tumor necrosis factor-α.

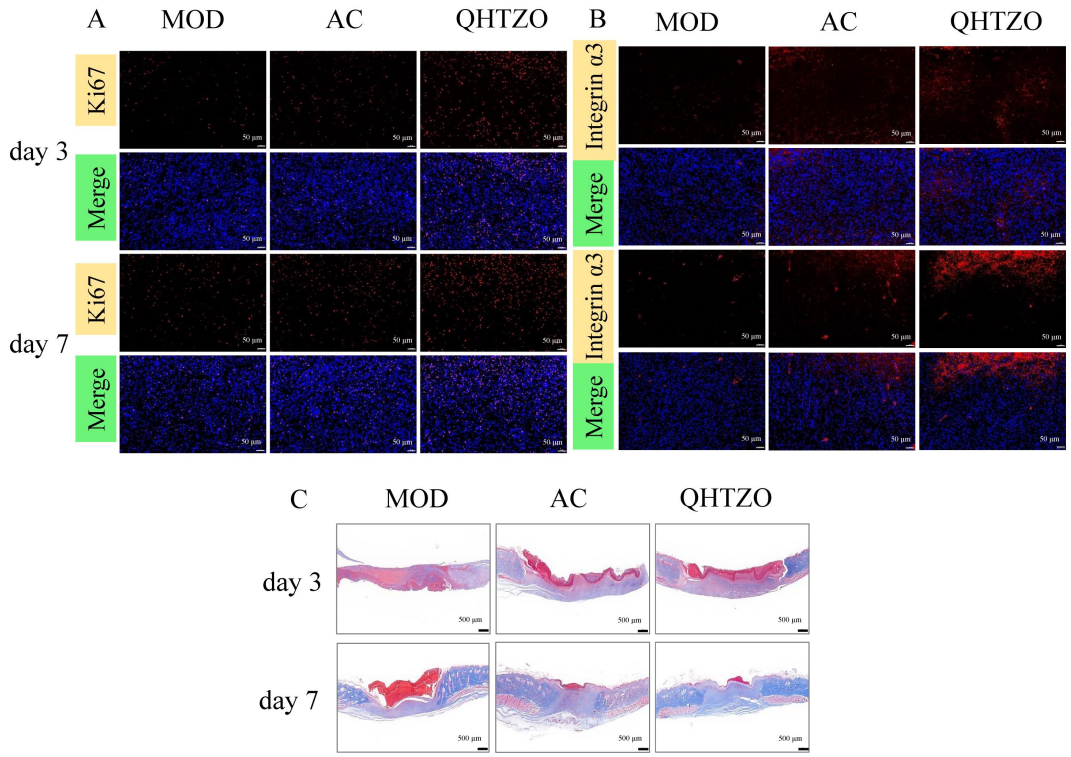

Figure 9 QHTZO enhances re-epithelialization, collagen deposition, and angiogenesis. (A) Representative immunofluorescence staining of Ki67 (green) and DAPI (blue) in wound area (scale bar = 50 μm); (B) Histological sections of wound area in different groups labeled with integrin *α*3 (red) and DAPI (blue) (scale bar = 50 μm); (C) Morphological observation on days 3 and 7 by Masson's trichrome staining (scale bar = 500 μm). QHTZO, Qi-Hong-Tang-Zu ointment.

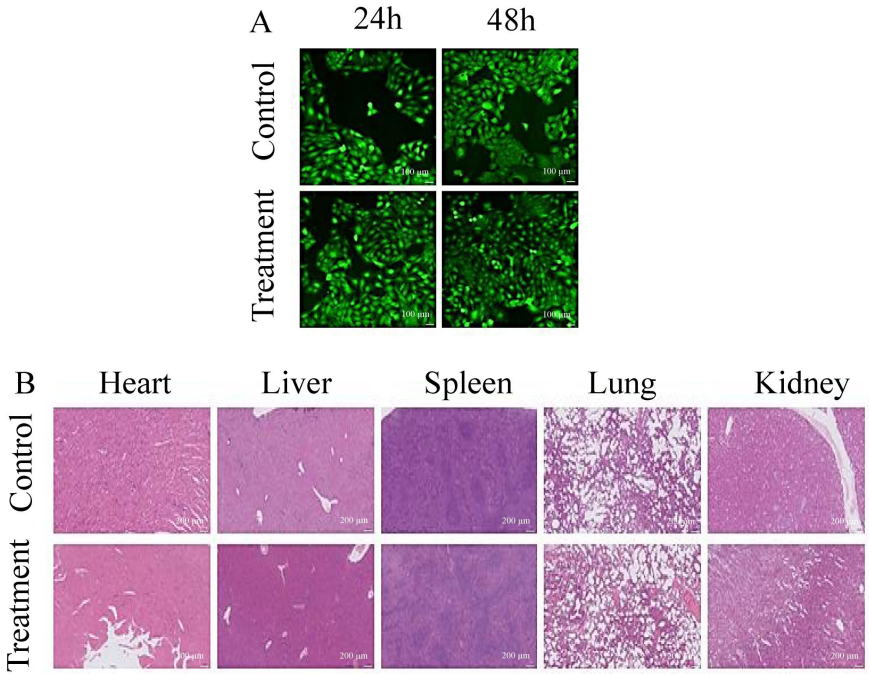

Figure 10 In vivo and in vitro safety evaluation. (A) Fluorescent staining images of HACAT cells after 24 h and 48 h of drug administration (scale bar = 100 μm); (B) Histological images of heart, liver, spleen, lung, and kidney stained with H&E after 10 d of treatment with QHTZO (healthy control) in diabetic wound rats (scale bar = 200 μm).

The research findings indicate that topical application of quercetin, possessing antioxidant and anti-inflammatory activities, promotes wound healing in incision and excision wounds of diabetic and non-diabetic rats. Results from cell and animal experiments suggest that total flavonoids of *Astragalus membranaceus* exert immunomodulatory and anti-inflammatory effects by regulating the MAPK and NF-κB signaling pathways in RAW246.7 macrophages [28]. In vitro experiments demonstrate a significant increase in cell proliferation when NIH3T3 cells are co-cultured with tannin-loaded nanospheres in a hydrogel [29].

The core targets involved in this study are *AKT1*, *IL-6*, *IL-1β*, and *EGFR*. *AKT1* regulates cell survival, proliferation, and angiogenesis,

induces glucose transport and uptake, and controls diabetes and its complications. Activated Akt increases the activity of the VEGF promoter and mediates the migratory response of endothelial cells to *VEGF* [30]. *EGFR* plays a critical role in the chemotaxis and proliferation of monocytes and macrophages. *EGFR* mediates cell proliferation, differentiation, and migration by signaling through epidermal growth factor, thereby regulating inflammatory responses, wound granulation, and neovascularization to promote wound healing.

KEGG enrichment mainly involves the AGE-RAGE signaling pathway, PI3K/Akt signaling pathway, and IL-17 signaling pathway. Studies have indicated that the AGE-RAGE signaling pathway is involved in regulating vascular neogenesis, tissue regeneration, and wound repair in diabetic foot ulcers. High blood glucose can activate the AGE-RAGE signaling pathway, affecting the oxidative stress level of diabetic foot ulcer wounds, while stimulating the expression and release of a large number of inflammatory factors, causing sustained damage and functional disruption in endothelial cells, impacting the integrity of blood vessel walls, and leading to vascular lesions [31]. The PI3K/Akt/mTOR signaling pathway plays an important regulatory role in the healing process of diabetic ulcers, as it can upregulate the expression of *VEGF*, *FGF*, and *EGF*, regulate cell migration, proliferation, differentiation, and apoptosis, induce epithelial-mesenchymal transition (EMT), and promote wound healing [32]. IL-17 can regulate the expression of pro-inflammatory genes, including inflammatory factors such as *IL-6*, *IL-1*, *TNF*, and *G-CSF*.

The molecular docking results revealed that quercetin, myricetin, and kaempferol have a Libdock score greater than 100 when binding with *IL-6* (*6MG1*), indicating a high affinity. *IL-6*, one of the most common inflammatory factors, is predominantly produced by monocytes, macrophages, T lymphocytes, and fibroblasts, with close interactions with the endocrine system [33, 34]. Previous research has established a significant association between IL-6 and diabetic complications [35].

IL-1β, *TNF-β*, *TNF-α*, and *IL-10* are inflammatory cytokines that play important roles in the early stages of wound healing. TNF-α and IL-1β secreted by M1 macrophages are associated with sustained pro-inflammatory responses that impede the healing process. In contrast, M2 macrophages produce anti-inflammatory and tissue repair-promoting factors such as *IL-10* and *TGF-β* [36]. Therefore, evaluating the levels of *IL-1β*, *TNF-β*, *TNF-α*, and *IL-10* in diabetic wound tissue is a key indicator for assessing the anti-inflammatory activity of the QHTZO. Experimental results indicate that QHTZO effectively inhibits the expression of pro-inflammatory cytokines (*TNF-α*, *IL-1β*) and promotes the expression of anti-inflammatory cytokines (*IL-10*, *TGF-β*). CD68 is a glycoprotein and serves as a marker for macrophages involved in wound healing. M1 macrophages overexpress CD80, CD86, and CD16/32, and secrete pro-inflammatory cytokines [37]. In this study, the QHTZO reduced the infiltration of M1 macrophages, promoted the infiltration of M2 macrophages into the wound, and alleviated local inflammation, thereby accelerating the healing of diabetic rat wounds.

Previously, major active ingredients such as myricetin, quercetin, and ellagic acid were identified in QHTZO by UPLC-Orbitrap-MS/MS analysis. These compounds may be the core pharmacological components in the TCM compound for intervening in diabetic foot. Research has shown that myricetin is a common plant flavonoid compound with a wide range of biological activities, including antioxidant, anticancer, antidiabetic, antihypertensive, antiallergic, and anti-inflammatory effects [38]. Myricetin isolated from *Tecomaria capensis v. aurea* has been studied for its local healing ability in wounds of albino rats. Myricetin can reduce the expression levels of pro-inflammatory cytokines (*IL-1β*, *TNF-α*) in rat serum and increase the expression of CD68. Myricetin can also inhibit the production of pro-inflammatory factors (*IL-6*, *IL-8*) in LPS-stimulated skin cells and decrease the expression level of MMP-1 in fibroblasts [39, 40]. In conclusion, myricetin can better improve wound healing in rats and can serve as an effective anti-inflammatory agent. Tetramethylpyrazine, a natural alkaloid found in chuanxiong, has been shown in modern pharmacology to promote diabetic wound recovery by polarizing macrophages from M1 to M2 phenotype [41]. In addition, quercetin has been found to inhibit inflammatory reactions by modulating macrophage polarization from the M1 to M2 phenotype, thereby speeding up diabetic wound repair [42]. Studies have also shown that wounds treated with quercetin exhibited increased collagen fiber content and decreased expression of inflammatory cytokines (*TNF-α*, *IL-1β*, and *IL-6*) [43]. Ellagic acid belongs to the flavonoid class of compounds, and previous studies have suggested that flavonoids play a role in wound healing. Research has shown that local application of ellagic acid, which possesses antioxidant and anti-inflammatory activities, promotes wound healing in both diabetic and non-diabetic rats [28]. Therefore, the TCM compound developed in this study, containing these active components, shows potential for the treatment of diabetic wounds.

The expression level of Ki67 serves as a marker of cell proliferation activity, with higher Ki67 levels indicating increased numbers of cells in the division phase and enhanced cell proliferation [44]. The study demonstrates that QHTZO promotes the expression levels of Ki67, facilitating wound healing. Keratinocytes, the main cell type in the epidermis, express and secrete a large number of growth factors, cytokines, and keratin, playing a vital role in wound healing. *Astragalus membranaceus* and *Rehmannia glutinosa* extract effectively promote the proliferation of keratinocytes by regulating the expression of growth factor receptors [45]. Research has found that the flavonoid compound quercetin has significant oxidative stress improvement effects. It regulates the expression of cytokines and growth factors, promotes fibroblast proliferation, angiogenesis, and collagen deposition, thereby accelerating wound healing [46]. Astragaloside IV promotes collagen deposition, expression of extracellular matrix-related genes (such as fibronectin and collagen IIIa), VEGF, and vWF in diabetic mice wounds, thereby promoting neovascularization and inducing alternative activated macrophage development, potentially playing a role in maintaining skin homeostasis and accelerating diabetic wound healing [47].

There are still some limitations in this study, as further experimental validation of the results from network pharmacology analysis was not conducted. To reflect the therapeutic effects of the traditional Chinese medicine compound ointment on diabetic wounds, more diversified methods can be utilized, such as increasing in vitro studies and deepening the exploration of mechanisms.

Conclusion

In conclusion, it has been elucidated that the core formula may exert therapeutic effects on diabetic wounds by targeting *AKT1*, *TNF*, *IL6*, *TP53*, *IL-1β*, *EGFR*, and other key points through components such as quercetin, naringenin, myricetin, kaempferol, ellagic acid, and isoquercitrin, and acting through signaling pathways including the PI3K-Akt pathway, cancer-related signaling pathways, and the AGE-RAGE signaling pathway. In addition, QHTZO can regulate the expression of *TGF-β*, *IL-10*, *IL-1β*, and *TNF-α*, as well as modulate macrophage polarization, reducing pro-inflammatory conditions in the body, enhancing the body's healing ability, promoting skin cell proliferation and collagen synthesis, thus showing good therapeutic effects on diabetic rats' wound.

References

1. Kautzky-Willer A, Harreiter J, Pacini G. Sex and Gender Differences in Risk, Pathophysiology and Complications of Type 2 Diabetes Mellitus. *Endocr Rev*. 2016;37(3):278–316. Available at: http://doi.org/10.1210/er.2015-1137
2. Sun YX, Tao Q, Wu XQ, Zhang L, Liu Q, Wang L. The Utility of Exosomes in Diagnosis and Therapy of Diabetes Mellitus and Associated Complications. *Front Endocrinol (Lausanne)*. 2021;12:756581. Available at: http://doi.org/10.3389/fendo.2021.756581

3. Wang HZ, Zhang LM. Intelligent biobased hydrogels for diabetic wound healing: A review. *Chem Eng J.* 2024;484:149493. Available at: http://doi.org/10.1016/j.cej.2024.149493
4. Zhang S, Ge G, Qin Y, et al. Recent advances in responsive hydrogels for diabetic wound healing. *Mater Today Bio.* 2022;18:100508. Available at: http://doi.org/10.1016/j.mtbio.2022.100508
5. Lin HT, Venault A, Chang Y. Zwitterionized chitosan based soft membranes for diabetic wound healing. *J Membr Sci.* 2019;591:117319. Available at: http://doi.org/10.1016/j.memsci.2019.117319
6. Chang M. Restructuring of the extracellular matrix in diabetic wounds and healing: A perspective. *Pharmacol Res.* 2016;107:243–248. Available at: http://doi.org/10.1016/j.phrs.2016.03.008
7. Liu J, Qu M, Wang C, et al. A Dual-Cross-Linked Hydrogel Patch for Promoting Diabetic Wound Healing. *Small.* 2022;18(17):e2106172. Available at: http://doi.org/10.1002/smll.202106172
8. Hu Y, Lei S, Yan Z, et al. Angelica Dahurica Regulated the Polarization of Macrophages and Accelerated Wound Healing in Diabetes: A Network Pharmacology Study and In Vivo Experimental Validation. *Front Pharmacol.* 2021;12:678713. Available at: http://doi.org/10.3389/fphar.2021.678713
9. Louiselle AE, Niemiec SM, Zgheib C, Liechty KW. Macrophage polarization and diabetic wound healing. *Transl Res.* 2021;236:109–116. Available at: http://doi.org/10.1016/j.trsl.2021.05.006
10. Amoupour M, Brouki Milan P, Barati M, et al. Suppression of SOCS3 expression in macrophage cells: Potential application in diabetic wound healing. *Int J Biol Macromol.* 2024;262(Pt 1):129876. Available at: http://doi.org/10.1016/j.ijbiomac.2024.129876
11. Al Sadoun H. Macrophage Phenotypes in Normal and Diabetic Wound Healing and Therapeutic Interventions. *Cells.* 2022;11(15):2430. Available at: http://doi.org/10.3390/cells11152430
12. Wu Y, Lyu Y, Li L, et al. Unimolecular Cascaded Multienzyme Conjugates Modulate the Microenvironment of Diabetic Wound to Promote Healing. *Biomacromolecules.* 2024;25(1):43–54. Available at: http://doi.org/10.1021/acs.biomac.3c00698
13. Pu Y, Wang P, Yang R, et al. Bio-fabricated nanocomposite hydrogel with ROS scavenging and local oxygenation accelerates diabetic wound healing. *J Mater Chem B.* 2022;10(21):4083–4095. Available at: http://doi.org/10.1039/D2TB00343K
14. Eming SA, Martin P, Tomic-Canic M. Wound repair and regeneration: Mechanisms, signaling, and translation. *Sci Transl Med.* 2014;6(265):265sr6. Available at: http://doi.org/10.1126/scitranslmed.3009337
15. Knoedler S, Knoedler L, Kauke-Navarro M, et al. Regulatory T cells in skin regeneration and wound healing. *Mil Med Res.* 2023;10(1):49. Available at: http://doi.org/10.1186/s40779-023-00484-6
16. Wu H, Li F, Shao W, Gao J, Ling D. Promoting Angiogenesis in Oxidative Diabetic Wound Microenvironment Using a Nanozyme-Reinforced Self-Protecting Hydrogel. *ACS Cent Sci.* 2019;5(3):477–485. Available at: http://doi.org/10.1021/acscentsci.8b00850
17. Ning SY, Zang J, Zhang BY, Feng XC, Qiu F. Botanical Drugs in Traditional Chinese Medicine With Wound Healing Properties. *Front Pharmacol.* 2022;13:885484. Available at: http://doi.org/10.3389/fphar.2022.885484
18. Paul-Traversaz M, Umehara K, Watanabe K, Rachidi W, Sève M, Souard F. Kampo herbal ointments for skin wound healing. *Front Pharmacol.* 2023;14:1116260. Available at: http://doi.org/10.3389/fphar.2023.1116260
19. Jin SM, Zhang MX, Gao Y, Zhang XB, Cui GZ, Zhang YJ. The Efficacy of Jing Wan Hong Ointment for Nerve Injury Diabetic Foot Ulcer and Its Mechanisms. *J Diabetes Res.* 2014;2014:259412. Available at: http://doi.org/10.1155/2014/259412
20. Fang L, Chen L, Song M, et al. Naoxintong accelerates diabetic wound healing by attenuating inflammatory response. *Pharm Biol.* 2021;59(1):252–261. Available at: http://doi.org/10.1080/13880209.2021.1877735
21. Zhao LL, Niu LJ, Liang HZ, Tan H, Liu CZ, Zhu FY. pH and Glucose Dual-Responsive Injectable Hydrogels with Insulin and Fibroblasts as Bioactive Dressings for Diabetic Wound Healing. *ACS Appl Mater Interfaces.* 2017;9(43):37563–37574. Available at: http://doi.org/10.1021/acsami.7b09395
22. Chen C, Wang Y, Zhang H, et al. Responsive and self-healing structural color supramolecular hydrogel patch for diabetic wound treatment. *Bioact Mater.* 2022;15:194–202. Available at: http://doi.org/10.1016/j.bioactmat.2021.11.037
23. Xu X, Guo Y, Chen M, et al. Hypoglycemic activities of flowers of Xanthoceras sorbifolia and identification of anti-oxidant components by off-line UPLC-QTOF-MS/MS-free radical scavenging detection. *Chin Herb Med.* 2023;16(1):151–161. Available at: http://doi.org/10.1016/j.chmed.2022.11.009
24. Shakhakarmi K, Seo JE, Lamichhane S, Thapa C, Lee S. EGF, a veteran of wound healing: highlights on its mode of action, clinical applications with focus on wound treatment, and recent drug delivery strategies. *Arch Pharm Res.* 2023;46(4):299–322. Available at: http://doi.org/10.1007/s12272-023-01444-3
25. Yadav JP, Singh AK, Grishina M, et al. Insights into the mechanisms of diabetic wounds: pathophysiology, molecular targets, and treatment strategies through conventional and alternative therapies. *Inflammopharmacology.* 2024;32(1):149–228. Available at: http://doi.org/10.1007/s10787-023-01407-6
26. Yang D, Tan YM, Zhang Y, et al. Sheng-ji Hua-yu ointment ameliorates cutaneous wound healing in diabetes via up-regulating CCN1. *J Ethnopharmacol.* 2023;303:115954. Available at: http://doi.org/10.1016/j.jep.2022.115954
27. Lin Y, Xu L, Lin H, et al. Network pharmacology and experimental validation to investigate the mechanism of Nao-Ling-Su capsule in the treatment of ischemia/reperfusion-induced acute kidney injury. *J Ethnopharmacol.* 2024;326:117958. Available at: http://doi.org/10.1016/j.jep.2024.117958
28. Fan SY, Shi XL, Wang AN, Hou TJ, Li K, Diao YP. Evaluation of the key active ingredients of 'Radix Astragali and Rehmanniae Radix Mixture' and related signaling pathways involved in ameliorating diabetic foot ulcers from the perspective of TCM-related theories. *J Biomed Inform.* 2021;123:103904. Available at: http://doi.org/10.1016/j.jbi.2021.103904
29. Kabirian KK, Tamri P, Haddadi R, Pourmoslemi S. Ellagic acid loaded nanospheres/biodegradable PVA-sodium alginate hydrogel for wound healing application. *J Appl Polym Sci.* 2023;140(37):e54406. Available at: http://doi.org/10.1002/app.54406
30. Geng J, Zhou G, Guo S, Ma C, Ma J. Underlying Mechanism of Traditional Herbal Formula Chuang-Ling-Ye in the Treatment of Diabetic Foot Ulcer through Network Pharmacology and Molecular Docking. *Curr Pharm Des.* 2024;30(6):448–467. Available at: http://doi.org/10.2174/0113816128287155240122121553
31. Wang Q, Zhu GY, Cao XZ, Dong JY, Song F, Niu YW. Blocking AGE-RAGE Signaling Improved Functional Disorders of

Macrophages in Diabetic Wound. *J Diabetes Res.* 2017;2017:1428537. Available at: http://doi.org/10.1155/2017/1428537
32. Deng H, Li B, Shen Q, et al. Mechanisms of diabetic foot ulceration: A review. *J Diabetes.* 2023;15(4):299–312. Available at: http://doi.org/10.1111/1753-0407.13372
33. Noel JG, Ramser SW, Pitstick L, et al. IL-1/MyD88–Dependent G-CSF and IL-6 Secretion Mediates Postburn Anemia. *J Immunol.* 2023;210(7):972–980. Available at: http://doi.org/10.4049/jimmunol.2200785
34. Kaur S, Bansal Y, Kumar R, Bansal G. A panoramic review of IL-6: Structure, pathophysiological roles and inhibitors. *Bioorg Med Chem.* 2020;28(5):115327. Available at: http://doi.org/10.1016/j.bmc.2020.115327
35. Forcina L, Franceschi C, Musarò A. The hormetic and hermetic role of IL-6. *Ageing Res Rev.* 2022;80:101697. Available at: http://doi.org/10.1016/j.arr.2022.101697
36. Yu Q, Shen Y, Xiao F, et al. Yuhong ointment ameliorates inflammatory responses and wound healing in scalded mice. *J Ethnopharmacol.* 2023;306:116118. Available at: http://doi.org/10.1016/j.jep.2022.116118
37. Yunna C, Mengru H, Lei W, Weidong C. Macrophage M1/M2 polarization. *Eur J Pharmacol.* 2020;877:173090. Available at: http://doi.org/10.1016/j.ejphar.2020.173090
38. Qian JQ, Zhang JQ, Chen Y, Dai CE, Fan J, Guo H. Hypoglycemic activity and mechanisms of myricetin. *Nat Prod Res.* 2022;36(23):6177–6180. Available at: http://doi.org/10.1080/14786419.2022.2058941
39. Elshamy AI, Ammar NM, Hassan HA, et al. Topical Wound Healing Activity of Myricetin Isolated from Tecomaria capensis v. aurea. *Molecules.* 2020;25(21):4870. Available at: http://doi.org/10.3390/molecules25214870
40. Trinh XT, Long NV, Van Anh LT, et al. A Comprehensive Review of Natural Compounds for Wound Healing: Targeting Bioactivity Perspective. *Int J Mol Sci.* 2022;23(17):9573. Available at: http://doi.org/10.3390/ijms23179573
41. Chu D, Chen J, Liu X, et al. A tetramethylpyrazine-loaded hyaluronic acid-based hydrogel modulates macrophage polarization for promoting wound recovery in diabetic mice. *Int J Biol Macromol.* 2023;245:125495. Available at: http://doi.org/10.1016/j.ijbiomac.2023.125495
42. Fu J, Huang J, Lin M, Xie T, You T. Quercetin Promotes Diabetic Wound Healing via Switching Macrophages From M1 to M2 Polarization. *J Surg Res.* 2020;246:213–223. Available at: http://doi.org/10.1016/j.jss.2019.09.011
43. Bains VK, Bains R. The antioxidant master glutathione and periodontal health. *Dent Res J (Isfahan).* 2015;12(5):389–405. Available at: http://doi.org/10.4103/1735-3327.166169
44. Yang JY, Chen ZY, Pan DY, Li HZ, Shen J. Umbilical Cord-Derived Mesenchymal Stem Cell-Derived Exosomes Combined Pluronic F127 Hydrogel Promote Chronic Diabetic Wound Healing and Complete Skin Regeneration. *Int J Nanomedicine.* 2020;15:5911–5926. Available at: http://doi.org/10.2147/ijn.s249129
45. Ren JW, Chan KM, Lai PK, et al. Extracts from Radix Astragali and Radix Rehmanniae Promote Keratinocyte Proliferation by Regulating Expression of Growth Factor Receptors. *Phytother Res.* 2012;26(10):1547–1554. Available at: http://doi.org/10.1002/ptr.4615
46. Kant V, Jangir BL, Kumar V, Nigam A, Sharma V. Quercetin accelerated cutaneous wound healing in rats by modulation of different cytokines and growth factors. *Growth Factors.* 2020;38(2):105–119. Available at: http://doi.org/10.1080/08977194.2020.1822830
47. Luo X, Huang P, Yuan B, et al. Astragaloside IV enhances diabetic wound healing involving upregulation of alternatively activated macrophages. *Int Immunopharmacol.* 2016;35:22–28. Available at: http://doi.org/10.1016/j.intimp.2016.03.020